Charge and spin transport in two-dimensional materials and their heterostructures

Bettadahalli Nandishaiah, Madhushankar

DOI:
10.33612/diss.135800814

2 Two-dimensional materials

Abstract

In this chapter, the basic structural and electronic properties of two-dimensional materials used in this thesis are introduced; these include germanane, graphene (single and bi-layer), transition metal di-chalcogenides (WS_2, WSe_2), and their heterostructures. The lattice structure of single atomic layers of these two-dimensional materials and their stacking geometry on top of another two-dimensional material are briefly explained. Further, the electronic band structure and the electronic properties of these two-dimensional materials are discussed.

2.1 Germanane

Germanane (GeH) is a two-dimensional semiconducting material analogous to graphane. The crystal structure of GeH consists of a hexagonal lattice of germanium (Ge) atoms with hydrogen (H) atoms covalently bonding alternatively to every Ge atom, as shown in Figure 2.1-1. Multilayer GeH consists of single layers stacked on top of each other and held together by weak van der Waals force. GeH has been recently synthesised for the first time by Bianco et al.[1] using topochemical deintercalation of $CaGe_2$. Single-layer GeH shows a direct bandgap of about 1.59 eV determined by diffuse reflectance absorption spectroscopy[1]. The bandgap of GeH decreases with increasing number of layers owing to interlayer interactions; however, it still remains a direct bandgap even for multilayers[2]. The electron charge carrier mobility in GeH which is limited by electron-phonon scattering, was calculated to be around 20,000 $cm^2V^{-1}s^{-1}$ at room temperature[1].

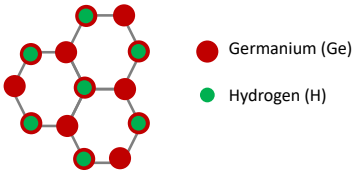

Figure 2.1-1 Lattice structure of the single-layer germanane (top view).

The top surface layer of GeH oxidises in contact with air over a period of five months and is self-limiting, i.e. it prevents the underlying layers from oxidizing. GeH is thermally stable up to a temperature of 75 ℃, and above this temperature amorphization occurs. The process of amorphization is complete at 175 ℃, and after, dehydrogenation is observed from a temperature of 200 to 250 ℃[1].

2.2 Graphene

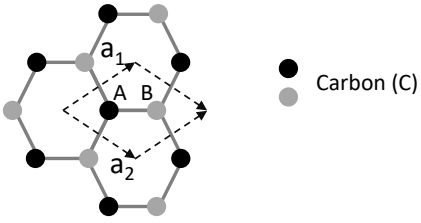

Figure 2.2-1 The hexagonal lattice structure of the single-layer graphene (top view), represented with two sub-lattices A and B which form the unit cell of graphene with lattice parameters a_1 and a_2.

Graphene is a two-dimensional allotrope of carbon; the carbon atoms are arranged in a hexagonal chick wire mesh configuration, as shown in Figure 2.2-1. Each carbon atom is covalently bonded to three of its neighbouring carbon atoms via σ bond while one π bond is oriented in the out-of-plane direction. The orbitals of the carbon atoms are sp^2 hybridised; a combination of s, p_x and p_y orbitals constituting the σ bond and the p_z orbital forming the π

bond. Each atomic layer is stacked on top of another held together by a weak van der Waals force.

The hexagonal structure of the graphene can be described as a triangular lattice with an unit cell containing two atoms A and B, as shown in Figure 2.2-1. Atoms A and B are chemically equivalent but they are different with respect to the lattice symmetry, and they form two inequivalent groups at the corners of the Brillouin zone that are labeled as K and K′ points in momentum space. From tight-binding calculations, the energy dispersion relation of the electrons close to Fermi energy in graphene is expressed as[3,4]:

$$E = \pm \hbar v_F |\vec{k}| \qquad \text{Equation 2.2-1}$$

where ħ is the reduced Planck constant, $\vec{k}$ is the wave vector, and $v_F \sim 10^6$ ms^{-1} is the Fermi velocity of electrons in graphene. Due to the linear dispersion, the band structure at K and K′ is cone-shaped which is inequivalent in the Brillouin zone. Graphene is a zero bandgap material since the conduction and the valence bands overlap with each other, the point of the overlap is known as the Dirac point. In addition to the spin degree of freedom, there exists a valley degree of freedom; both the valleys have the same energy but are inequivalent in k-space. The interesting electronic properties of the graphene are a result of this valley degenerate zero bandgap states. In comparison, for a conventional semiconductor like silicon, the main point of interest is generally Γ point in the Brillouin zone (Γ is the center of the Wigner-Seitz cell) where the momentum is zero.[5]

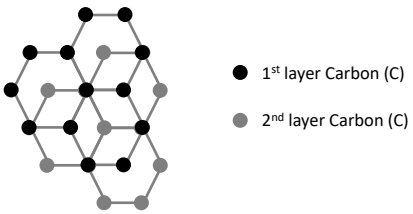

Figure 2.2-2 The lattice structure of a bi-layer graphene in AB-type stacking of two individual single-layer graphene flakes represented as 1st and 2nd layer (top view).

Bilayer graphene has two layers of graphene monolayers stacked on top of one another and held by a weak van der Waals force. The stacking geometry of the graphene layers in bilayer graphene can be either AB or AA type. In AB type, half of the carbon atoms in the upper layer lie directly over the centre of the hexagon in the lower graphene sheet, and the other half of the carbon atoms lie over the carbon atom from the lower layer[6], as shown in Figure 2.2-2. Whereas in AA type, the layers are exactly aligned with respect to each other[7]. AB stacked structure is much more stable in comparison to AA stacked geometry[7].

2.3 Transition metal di-chalcogenides

Transition metal di-chalcogenides (TMD) are a class of two-dimensional materials represented as MX_2; M is a transition metal which can either be Molybdenum (Mo) or Tungsten (W), and X is the chalcogenide which can either be Sulphur (S), or Selenide (Se),

or Tellurium (Te). Each of the metal (Mo or W) atom is covalently bonded to six chalcogenides (S, or Se, or Te) atoms in trigonal prismatic geometry, and each chalcogenide atom is bonded to three metal atoms in pyramidal geometry[8], as shown in Figure 2.3-1. Each layer of X-M-X is stacked on top of another with a weak van der Waals force. The TMDs studied in this thesis are tungsten di-sulphide (WS_2) and tungsten di-selenide (WSe_2).

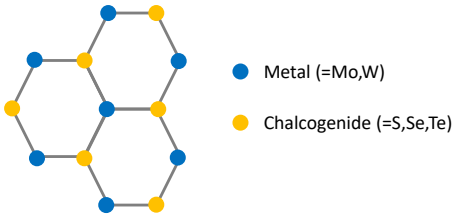

Figure 2.3-1 The hexagonal lattice structure of a single-layer transition metal di-chalcogenide (top view).

The TMDs are semiconducting with a direct bandgap for single layer and indirect bandgap for multilayers. For a monolayer TMD, the conduction and the valence band edges are located at non-equivalent K points (K and K′) of the two-dimensional hexagonal Brillouin zone. The charge (coupled to spins) transition between the valence and the conduction bands in the K and K′ valleys can be achieved by using a right and left circularly polarised light respectively. This valley dependent optical selection rule is due to the absence of inversion centre in a monolayer TMD (this also applies to TMD with odd number of layers). Further, the valence and the conduction bands at the K and K′ valleys are spin split due to a strong spin-orbit coupling, leading to coupling of the spin and valley degrees of freedom in a single layer TMD.

A single-layer of WS_2 has a direct band gap of 2 eV[9] and the multilayer of WS_2 has an indirect band gap[9] of about 1 eV[9]. Similarly a single layer of WSe_2 has a direct band gap of 1.7 eV[9] and the multilayer of WSe_2 has an indirect band gap of about 1 eV[10]. Due to a strong spin-orbit coupling present in both WS_2 and WSe_2, spin splitting is observed in the order of hundreds of meV in the conduction band while few meV in the valence band at the K and K′ valleys[11]. The electron spins residing in these valleys can be excited by tuning the photon energy of the excitation laser and by tuning its handedness (right or left circularly polarised light).

2.4 Graphene-TMD heterostructure

In the context of spintronics, graphene has a long spin diffusion length[12] because of its low spin-orbit coupling (SOC) in the order of 10 μeV[13]. However, this magnitude of SOC is ineffective in generation and manipulation of spin current. Transition metal di-chalcogenides like WS_2 and WSe_2 have strong intrinsic SOC. By placing these TMDs in the proximity of graphene, one can induce strong SOC in graphene. Further, by placing TMD with graphene, the inversion symmetry in graphene is broken. These effects, the induced SOC and the breaking of inversion symmetry, open up a band gap in graphene with spin split and valley locked states.

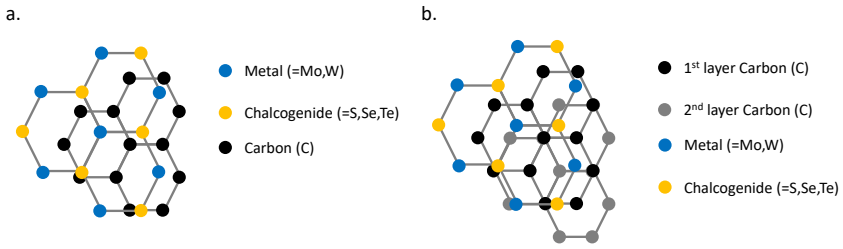

Figure 2.4-1 The overlapping lattice structures of (a) single layer graphene in proximity with TMD, and (b) bi-layer graphene in proximity with TMD (top view).

The TMD can be easily stacked on top of graphene (or below) to form van der Waals heterostructures as shown in Figure 2.4-1. However, in these heterostructures, there is a mismatch in the lattice constants (a) of graphene and TMD; graphene has a = 2.46 Å whereas WSe_2 has a = 3.29 Å. Further, in the stacks of graphene/TMD prepared and presented in this thesis, we could not control the crystal orientation of either the graphene or the WSe_2 with respect to each other.

Detailed theoretical and experimental studies on single and bi-layer graphene in proximity with TMD are discussed in chapters 3.7, 6, 7 and 8 of this thesis.

References

1. Bianco, E. et al. Stability and Exfoliation of Germanane: A Germanium Graphane Analogue. ACS Nano **7**, 4414–4421 (2013).

2. Shu, H., Li, Y., Wang, S. & Wang, J. Thickness-Dependent Electronic and Optical Properties of Bernal-Stacked Few-Layer Germanane. J. Phys. Chem. C **119**, 15526–15531 (2015).

3. Wallace, P. R. The Band Theory of Graphite. Phys. Rev. **71**, 622–634 (1947).

4. Castro Neto, A. H., Guinea, F., Peres, N. M. R., Novoselov, K. S. & Geim, A. K. The electronic properties of graphene. Rev. Mod. Phys. **81**, 109–162 (2009).

5. Daniel R. Cooper, Benjamin D'Anjou, Nageswara Ghattamaneni, Benjamin Harack, Michael Hilke, Alexandre Horth, Norberto Majlis, Mathieu Massicotte, Leron Vandsburger, Eric Whiteway, and V. Y. Experimental Review of Graphene. Condens. Matter Phys. **2012**, 56 pages (2012).

6. Yan, K., Peng, H., Zhou, Y., Li, H. & Liu, Z. Formation of Bilayer Bernal Graphene: Layer-by-Layer Epitaxy via Chemical Vapor Deposition. Nano Lett. **11**, 1106–1110 (2011).

7. Liu, Z., Suenaga, K., Harris, P. J. F. & Iijima, S. Open and Closed Edges of Graphene Layers. Phys. Rev. Lett. **102**, 15501 (2009).

8. Liu, G.-B., Xiao, D., Yao, Y., Xu, X. & Yao, W. Electronic structures and theoretical modelling of two-dimensional group-VIB transition metal dichalcogenides. Chem. Soc. Rev. **44**, 2643–2663 (2015).

9. Yun, W. S., Han, S. W., Hong, S. C., Kim, I. G. & Lee, J. D. Thickness and strain effects on electronic structures of transition metal dichalcogenides: 2H-MX2 semiconductors (M=Mo, W; X=S, Se, Te). Phys. Rev. B **85**, 33305 (2012).

10. Prakash, A. & Appenzeller, J. Bandgap Extraction and Device Analysis of Ionic Liquid Gated WSe2 Schottky Barrier Transistors. ACS Nano **11**, 1626–1632 (2017).

11. Kosmider, K., González, J. W. & Fernández-Rossier, J. Large spin splitting in the conduction band of transition metal dichalcogenide monolayers. Phys. Rev. B **88**, 245436 (2013).

12. Drögeler, M. et al. Spin Lifetimes Exceeding 12 ns in Graphene Nonlocal Spin Valve Devices. Nano Lett. **16**, 3533–3539 (2016).

13. Gmitra, M., Konschuh, S., Ertler, C., Ambrosch-Draxl, C. & Fabian, J. Band-structure topologies of graphene: Spin-orbit coupling effects from first principles. Phys. Rev. B **80**, 235431 (2009).